Biochimica et Biophysica Acta 1808 (2011) 2954–2964

Contents lists available at ScienceDirect

Biochimica et Biophysica Acta

journal homepage: www.elsevier.com/locate/bbamem

ATP hydrolysis at one of the two sites in ABC transporters initiates transport related conformational transitions

Gergely Gyimesi [a,b], Srinivas Ramachandran [c], Pradeep Kota [c], Nikolay V. Dokholyan [c], Balázs Sarkadi [a], Tamás Hegedűs [a,b,*]

[a] Membrane Research Group, Hungarian Academy of Sciences, Budapest, Hungary
[b] Department of Biophysics, Semmelweis University, Budapest, Hungary
[c] Department of Biochemistry and Biophysics, UNC, Chapel Hill, NC, USA

ARTICLE INFO

Article history:
Received 15 March 2011
Received in revised form 23 June 2011
Accepted 25 July 2011
Available online 3 August 2011

Keywords:
ABC transporter
Molecular dynamic
Membrane bilayer
Multi-drug resistance
Constant contact model

ABSTRACT

ABC transporters play important roles in all types of organisms by participating in physiological and pathological processes. In order to modulate the function of ABC transporters, detailed knowledge regarding their structure and dynamics is necessary. Available structures of ABC proteins indicate three major conformations, a nucleotide-bound "bottom-closed" state with the two nucleotide binding domains (NBDs) tightly closed, and two nucleotide-free conformations, the "bottom-closed" and the "bottom-open", which differ in the extent of separation of the NBDs. However, it remains a question how the widely open conformation should be interpreted, and whether hydrolysis at one of the sites can drive conformational transitions while the NBDs remain in contact. To extend our knowledge, we have investigated the dynamic properties of the Sav1866 transporter using molecular dynamics (MD) simulations. We demonstrate that the replacement of one ATP by ADP alters the correlated motion patterns of the NBDs and the transmembrane domains (TMD). The results suggest that the hydrolysis of a single nucleotide could lead to extracellular closure, driving the transport cycle. Essential dynamics analysis of simulations suggests that single nucleotide hydrolysis can drive the system toward a "bottom-closed" apo conformation similar to that observed in the structure of the MsbA transporter. We also found significant structural instability of the "bottom-open" form of the transporters in simulations. Our results suggest that ATP hydrolysis at one of the sites promotes transport related conformational changes leading to the "bottom-closed" apo conformation, which could thus be physiologically more relevant for describing the structure of the apo state.

1. Introduction

ABC (ATP Binding Cassette) transmembrane proteins play important roles in translocating a broad class of substrates across biological membranes in all types of organisms [1]. The failure of ABC proteins to translocate their physiological substrates results in different kinds of human diseases, including cystic fibrosis, Dubin-Johnson syndrome, diabetes mellitus type II, and adrenoleukodystrophy (http://nutrigene.4t.com/humanabc.htm). A very important phenomenon caused by some ABC transporters is multi-drug resistance of cancers against chemotherapeutic treatment [2–4]. Since some ABC proteins (e.g. MDR1, Multi-Drug Resistance protein 1; MRP1, Multi-drug Resistance associated Protein 1; ABCG2) have low substrate specificity and can remove compounds with various chemical properties from the cell, efflux of drugs through these transporters results in a decrease of drug concentration inside the cell below the effective level. The export process is driven by ATP binding and/or hydrolysis at the cytoplasmic nucleotide binding domains (NBD). The Walker A and B motifs are part of the core subdomain of NBD, while the α-helical region of the protein contains the ABC signature sequence [5,6]. Biochemical and structural studies have demonstrated that the binding of ATP to the Walker motifs in each NBD and to the signature sequence in the opposite NBD allows a tight association ("dimerization") of two NBDs [7,8]. In this ATP-bound holo state, the cytoplasmic parts of the transmembrane domains (TMD) are also close to each other, in a so called "bottom-closed" outward-facing conformation [9,10]. In the absence of nucleotides, X-ray structures indicate a "bottom-open" inward-facing conformation, where the NBDs are far from each other (Fig. 1 and S6) [10–12]. A region crucial for the transitions between the holo and apo conformations is the interface connecting the NBDs and TMDs. This interface contains short distal segments of intracellular loops,

Abbreviations: ABC, ATP Binding Cassette; NBD, nucleotide binding domain; TMD, transmembrane domain; ED, essential dynamics; ASA, accessible surface area

* Corresponding author at: Membrane Research Group, Hungarian Academy of Sciences, Tűzoltó u. 37-47, Budapest, 1097, Hungary. Tel./fax: +36 1 2676261, +36 1 2666656.
E-mail address: tamas@hegelab.org (T. Hegedűs).
URL: http://www.hegelab.org (T. Hegedűs).

0005-2736/$ – see front matter © 2011 Elsevier B.V. All rights reserved.
doi:10.1016/j.bbamem.2011.07.038

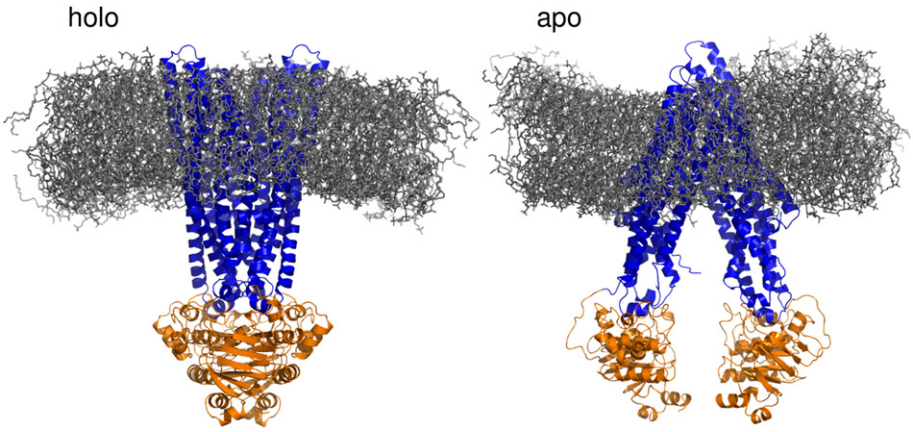

Fig. 1. The two key conformations of ABC transporters used in molecular dynamics simulations. The left panel shows the "bottom-closed" holo conformation of the Sav1866 bacterial transporter (PDB ID: 2HYD), which was used to study the effect of ATP to ADP replacement. On the right, the "bottom-open" apo conformation of the mouse MDR3 transporter (PDB ID: 3G5U) is shown, which was used for simulating the apo state. The structures in the figure are the initial conformations for the Sav1866 ATP/ATP and mouse MDR3 simulations, respectively, embedded in a POPC bilayer. Dark gray/blue: transmembrane domains, light gray/orange: nucleotide binding domains.

called coupling helices [9]. A coupling helix connects two anti-parallel helices, which are extensions of transmembrane helices, forming an intracellular "loop". The contact surface on the NBDs includes two main regions. One of them is the conserved X-loop, located C-terminal to the Walker A motif and N-terminal to the signature sequence [9]. The other is the Q-loop [13], which connects the α-helical subdomain containing the signature motif with the core subdomain and also interacts with the bound Mg^{2+} ion of ATP [7,14]. In the nucleotide-bound state, an important structural feature, which forms a significant part of the interface between the TMDs, is a tetra-helix bundle composed of the cytoplasmic parts of the TM3 and TM4 transmembrane helices of both transmembrane domains [15].

Understanding the coupling of ATP binding and/or hydrolysis to changes in the TMD conformation and substrate translocation is important for designing drugs to modulate transporter activity. The variety of available X-ray structures and drug binding studies have shown that ABC transporters are highly flexible [16], so a single static conformation, such as an X-ray crystal structure, might not be adequate to describe protein conformation and identify drug targets. Therefore, the dynamic properties of ABC proteins are being explored by both experimental and computational methods. Recently, electron paramagnetic resonance (EPR) spectroscopy has become a popular method to study the dynamics of this class of proteins [17–22]. EPR experiments with different conformations of the target protein are performed to measure distances between two spin labels attached to specifically selected amino acid pairs. Measuring distances between two specific residues by chemical cross-linking can be also used to derive information on protein conformation and dynamics [23–25]. However, both of these methods have limitations and do not provide atomic level information on the motions in the protein. In most cases these experimental methods provide only information on distances between two residues in the protein, and no directional information. In addition, while some experimental results reconcile with the wide opening of NBDs seen in some "bottom-open" X-ray structures [17], cross-linking studies with human MDR1 protein suggest that a large opening is not necessary for function [25].

To overcome this limitation of experimental methods, and to help interpret experimental data, molecular dynamics (MD) simulations have been used extensively to understand motions in ABC proteins at high resolution. Many computational studies have investigated the role of ATP in stabilizing the interactions between nucleotide binding domains in systems containing only these two cytoplasmic domains [26–31]. Simulations with NBD dimers or monomers with either ATP or ADP have shed light on the possible conformational changes induced by hydrolysis. Although there is no clear indication whether hydrolysis at one nucleotide binding site enhances or disrupts hydrolysis at the other site [30,31], most simulation results as well as half-open X-ray structures indicate that the helical domain of the *trans* NBD rotates outwards after ATP hydrolysis, facilitating nucleotide exchange [26,27]. This rotation would imply the concerted motion of the Q-loops and X-loops of the *trans* NBD, which have been shown experimentally to have an important role in signal transduction towards the TMD [32,33].

Few studies report simulations of full-length ABC proteins in a lipid environment, since sampling at biologically relevant time-scales in the case of such large proteins with lipids requires high computational power. The bacterial vitamin B12 importer (BtuCD) system has been extensively investigated using MD simulations. Using 15 ns long simulations with BtuCD in a lipid bilayer, ATP binding was shown to induce conformational changes in both NBDs and TMDs, indicating that the binding itself may be the power stroke in the catalytic cycle [34]. Elastic network normal mode analysis and biased molecular dynamics simulations have also been employed to predict the possible mechanism of transport of vitamin B12 [35]. BtuCD has been investigated in detail also by Ivetac et al. [36], whose molecular dynamics simulations combined with principal component analysis exhibited asymmetry in the ATP binding domain supporting the alternating hydrolysis mechanism [37] for ABC transporters. A recent simulation of the whole Sav1866 transporter has revealed a number of residues present at the NBD-TMD interface within the Q-loops and X-loops providing information at the atomic level how these regions could transmit conformational changes [14]. Until now, however, no systematic study has been carried out on the full pathway of conformational changes originating in the NBDs and transmitted to the TMDs. Possible pathways of transition from holo to apo conformation have been explored at atomic resolution using targeted MD simulations [15]. MD simulations also have been used to assess the global stability and structural integrity of ABC proteins [38], and have demonstrated that the now revoked structure of MsbA, whose X-ray structure had the correct transmembrane helices but an incorrect handedness and topology, suffered from large distortions even in short MD simulations.

In this study, we aim to characterize the dynamics of ABC proteins in different states, embedded in a lipid bilayer. First, long molecular dynamics simulations are performed with the holo Sav1866 X-ray structure in the presence of two ATP molecules and also one ATP and one ADP in the nucleotide binding domains, to describe the effect of ATP hydrolysis on the long range dynamics of the protein. Second, we also employ these simulations to characterize the transition of the

Sav1866 transporter from the holo to the apo conformation. Third, the instability of the "bottom-open" conformation is described in simulations of the mouse MDR3 structure.

Our results suggest that subtle changes in the dynamics of the "bottom-closed" conformation caused by one ADP replacement may be sufficient to drive the transport process. Although these simulations challenge the proposed mechanistic view of ABC transport cycle based on the inward- and outward-facing conformations observed in crystals and advocate the alternating sites model of mechanism, they may help us in understanding the structure and dynamics necessary for the function of ABC proteins.

2. Methods

2.1. Structural models

2.1.1. Nucleotide-bound form of Sav1866

The structure of Sav1866 co-crystallized with bound ADP was used (PDB ID: 2HYD) for simulations. MgATP was constructed from the MJ0796 dimer X-ray structure (PDB ID: 1L2T) by RMSD fitting the protein structure to the Sav1866 structure and transferring the γ-phosphate group, the Mg^{2+} ion and coordinating water molecules. The resulting Sav1866 ATP/ATP and ATP/ADP structures were subject to energy minimization using the steepest descent algorithm and an emtol value of 500 kJ mol^{-1} nm^{-1} (GROMACS 4.0.3 [39]). The relaxed complex structures were used for membrane insertion.

2.1.2. Homology model of the nucleotide-bound form of mMDR3

To compare the accessible surface are of the apo and holo conformations of mMDR3, a homology model of the mMDR3 holo form was created with MODELLER 9v7 [40] using the structure of Sav1866 as a template (PDB ID: 2HYD). Pairwise sequence alignment was generated using ClustalW [41] with the default settings. The alignment was modified by hand to cause large insertions to fall on the region of extracellular loops, similarly to [42]. The best model according to the objective function of MODELLER was selected.

2.2. Molecular dynamics simulations

Proteins were solvated in a box of SPC water and an equilibrated lipid bilayer. The accuracy of protein placement in the membrane is crucial, however, transmembrane helix predictors do not perform well on ABC transporter sequences, and some of the software even predicts a different number of transmembrane helices for an ABC protein than confirmed by experiments. Therefore, we used both sequence-based and structure-based methods (HMMTOP [43] and TMDET [44], respectively) to guide the insertion of our structures into the bilayer (Fig. 1). After inserting our models into the membrane, the hydrophobic sides of the N-terminal amphipathic helices ("elbow" helices) are in close contact with the inner leaflet of the bilayer indicating the appropriateness of the insertion. The gap between the solvated protein and the lipid molecules was filled up by a series of simulations. The first fill-up simulation lasted for 20 ns with harmonic position restraints forcing the protein atoms to their initial positions with a force constant of 1000 kJ mol^{-1} nm^{-2}. This was followed by three similar simulations of 200 ps decreasing the force constant between simulations in steps of 250 kJ mol^{-1} nm^{-2}. The production runs were performed without any position restraints. The Sav1866 ATP/ATP and ATP/ADP simulations were performed using the GROMOS96 G53a6 force field in POPC bilayer using surface-tension pressure coupling with a surface tension of zero and a *z*-compressibility of 4.5×10^{-5} bar^{-1}. The first two simulations of each system were 100 ns long. To enhance sampling, three shorter simulations of 50 ns each were also performed, resulting in a total of 5 simulations for each system. The mouse MDR3 apo structure was used for three independent simulations of 100 ns each, with the same parameters. Due to the instability of the mouse MDR3 protein in our simulations, other parameters were also tested (Table 1). For all simulations, velocity rescaling thermostat was used at a temperature of 310 K. MD simulations were performed using GROMACS 4.0.3 [39].

2.3. Analysis

2.3.1. RMSD, essential dynamics (ED) and flexibility analysis

RMSD analysis employed only C_α atoms of structures. Essential dynamics analysis was performed by fitting all structures after 20 ns from the two 100 ns simulations of the Sav1866 ATP/ADP system on the initial conformation (in total 80,000 structures), then calculating the covariance matrix of atomic positions and its eigenvectors and eigenvalues. The fitting was performed using only the TMDs (residues 1–318), and only C_α atoms were used in the calculation. RMS fluctuation calculations used the average RMS value for all atoms in each residue, from time frames in the first 50 ns of each Sav1866 simulation, yielding in total 5–5 values per residue. The average and standard deviation of the per residue RMS values were then calculated for the ATP/ATP and ATP/ADP system separately. These analyses were carried out using standard GROMACS tools.

2.3.2. Extracting mutual information from simulations with Sav1866

The MutInf method was used to calculate the mutual information between pairs of residues [45]. In this method, first, mutual information between pairs of dihedral angles are calculated as

$$I = S(1) + S(2) - S(1,2)$$

where $S(1)$ and $S(2)$ are the self-entropies of the two dihedrals and $S(1,2)$ is their joint entropy. These quantities are calculated using a 2D histogram method and employing various correction schemes for incomplete sampling in the dataset. The mutual information of a pair of residues was defined as the sum of all combination of pairs of their dihedral angles [45]. The MutInf program was kindly provided by the authors. For each system, 10,000 frames were used between 30 and 50 ns from all five simulations trajectories. Adaptive partitioning was used as in [45]. The network of residues was created by extracting all pairs of residues with mutual information above a certain threshold. The threshold was chosen to be $3k_B$ (k_B is the Boltzmann constant) to make the number of residues in the network fall in the range 25–50. Graphs were created using neato from the GraphViz package (http://www.graphviz.org).

2.3.3. Quantification of nucleotide binding site opening

The distance between the C_α atoms of Ser381A–Ser479B and Ser381B–Ser479A residue pairs that sandwich the bound nucleotide in site A and B, respectively, was calculated as a function of time. In Sav1866, Ser381 is part of the Walker A motif coordinating the bound Mg^{2+} ion, while Ser479 is the serine of the LSGGQ ABC signature motif, which is in contact with the γ-phosphate of ATP.

2.3.4. Secondary structure assessment and helical content calculation

Secondary structure prediction from 3D coordinates was done using DSSP [46] for each frame of the simulation trajectory. The dominant secondary structure for each residue was defined as one that is observed during at least 80% of the simulation time. The domain boundaries were defined as Met1–Asp319 (chain A and B) for Sav1866 TMD, Val35–Asn367 and Ser692–Glu1009 for mMDR3 TMD. The calculation was only performed for TMDs.

2.3.5. Calculating accessible surface area

The *surface* program, which uses the algorithm of Lee and Richards, was used from the CCP4 suite [47,48] to calculate the accessible surface area of each atom in the structures, using default values. The regions of intracellular loops in mMDR3 were defined as amino acids

Table 1
Systems and parameters used in the MD simulations.

Protein	Conformation	Lipids	Duration	Force field	Pressure coupling	z compressibility
Sav1866 + 2xATP	Holo	POPC	2 × 100 ns	GROMOS96	Surface-tension	4.5×10^{-5} bar^{-1}
Sav1866 + 2xATP	Holo	POPC	3 × 50 ns	GROMOS96	Surface-tension	4.5×10^{-5} bar^{-1}
Sav1866 + ATP/ADP	Holo	POPC	2 × 100 ns	GROMOS96	Surface-tension	4.5×10^{-5} bar^{-1}
Sav1866 + ATP/ADP	Holo	POPC	3 × 50 ns	GROMOS96	Surface-tension	4.5×10^{-5} bar^{-1}
mMDR3	Apo	POPC	3 × 100 ns	GROMOS96	Surface-tension	4.5×10^{-5} bar^{-1}
mMDR3	Apo	DPPC	70 ns	OPLS/AA	Surface-tension	0

133–181, 233–287, 351–373, 779–825, 878–934, and 998–1017. Hydrophobic amino acids were defined as Gly, Ala, Val, Leu, Ile, Met, Phe, Tyr, Trp and Pro, others were considered as hydrophilic.

3. Results

3.1. Systems used in MD simulations

Our major goal was to compare the dynamics of the holo and apo conformations of ABC transporters to elucidate the mechanism of conformational changes in the catalytic cycle, such as NBD opening and closure of the transmembrane helices. Therefore, we performed MD simulations using the "bottom-closed" Sav1866 (PDB ID: 2HYD) and the "bottom-open" mouse MDR3 (PDB ID: 3G5U) X-ray structures.

We performed our simulations in a membrane built from POPC (palmitoyl-oleoyl-phosphatidylcholine) using the GROMOS96 53a6 force field [49]. The quality of our lipid bilayer was checked by monitoring the average surface area per lipid of the bilayer, which varied between 67 Å^2 and 71 Å^2 for the Sav1866 simulations (Fig. S1). These values are consistent with the simulations used to validate the lipid parameters and are in good agreement with experimental values [50]. All of these measures indicate that the POPC bilayer in the simulations is stable and well-equilibrated.

While the "bottom-closed" conformations of Sav1866 were stable in all simulations, the "bottom-open" conformation of the mouse MDR3 protein has been indicated to be unstable with the GROMOS96 force fields (M. L. O'Mara, personal communication) and was also unstable in our simulations (see Section 3.5). Therefore, we tested the effect of different parameters (e.g. choice of lipids, pressure coupling, surface tension) and of force field choice (e.g. OPLS all-atom force field) in our simulations. The complete list of the different simulations performed can be found in Table 1.

3.2. Single ATP/ADP replacement changes correlated motion patterns

To explore the effects of ATP hydrolysis, we performed simulations of the "bottom-closed" conformation of the Sav1866 homodimer in POPC bilayer. The simulations ranged in length between 50 and 100 ns. The root mean square deviations (RMSD) of C_α atoms in the production runs exhibit values within 3–5 Å. Values in this range are higher than what might be expected for water soluble protein simulations, but they agree with other simulations of the same protein [14] indicating stable simulations (Fig. 2). We observed larger fluctuations in the TMDs (RMSD 3.5–4 Å) than among NBDs (2.5 Å), but all the domains retained their overall folds. MD runs were performed with ATP in both nucleotide binding sites (ATP/ATP) and with one ATP replaced by an ADP (ATP/ADP) to model the result of nucleotide hydrolysis in the site containing the Walker A motif of chain B (site B). Several independent simulations were performed using the same initial structure to enhance the sampling of conformational space (Table 1).

We applied the MutInf approach described by McClendon et al. [45] to the Sav1866 system to assess the change in the dynamics of the protein upon the modeled ATP hydrolysis. This method comprises a histogram based mutual information calculation of protein dihedral angles, and is able to detect concurrent conformational changes happening at an atomic scale in the protein. A high value of mutual information indicates a stronger dynamic coupling between two residues and can be used to find residues that take part in allosteric communication between two parts of the protein [45]. The advantage of the MutInf method over other methods is its enhancement of the signal/noise ratio using numerous corrections to filter out statistically insignificant correlations. The mutual information of dihedral angles for all residue pairs was calculated for both ATP/ATP and ATP/ADP containing simulations. To visualize the coupling between residues in a system containing both ATP and ADP, a network of highly correlated residues was constructed (Fig. 3).

The network of correlated residues in the case of the system containing ATP in both binding sites has a high number of edges showing extended connectivity (Fig. 3A). The residues are labeled by their type, number and chain identifier. Three groups of residues that are cliques (complete subgraphs) with more than three members can be observed, one containing the ATP-sensing residue Gln422B from chain B (Gln422B-Asp323B-Met311B-Asp312B), and two containing the

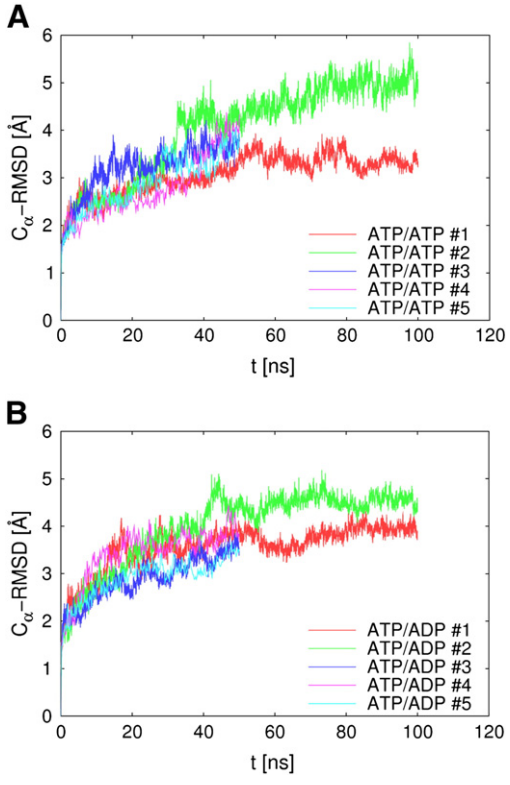

Fig. 2. Stability of the Sav1866 structure in simulations. The stability of the protein during the simulation was characterized by root mean square deviation (RMSD) from the initial structure which was used to start the production runs. RMSD values below 5–6 Å are generally considered being characteristic for a stable protein of this size in molecular dynamics simulations. Data is shown for the Sav1866 ATP/ATP (A) and ATP/ADP (B) containing simulations.

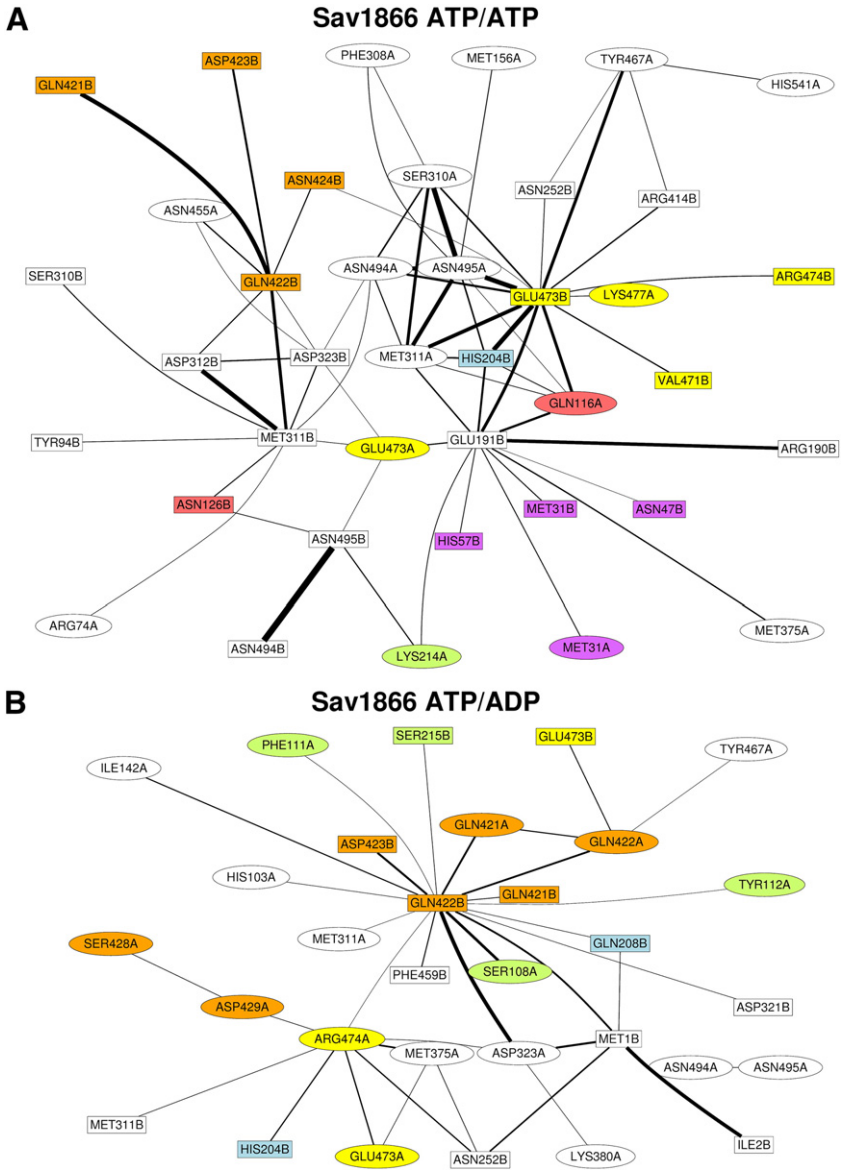

Fig. 3. Mutual information analysis indicates changes in correlated residue motions after replacing ATP to ADP in site B. The network of mutual information (MI) between residues displays marked differences between the Sav1866 ATP/ATP (A) and ATP/ADP (B) containing systems. Residues are connected if they share MI higher than $3k_B$ (see Methods). Edge width is proportional to the amount of MI. Residues in chain A and B are drawn as ellipses and rectangles, respectively. Colors indicate functionally important regions; yellow: X-loop (469–477), orange: Q-loop (421–430), red: TM3 region of the tetra-helix bundle (116–127), blue: TM4 region of the tetrahelix bundle (193–208), green: coupling helices (107–116, 209–218), violet: residues accessible from the extracellular side (31, 47, 57).

conserved Glu473B residue (Glu473B-Ser310A-Asn494A-Met311A-Asn495A and Glu473B-Gln116A-Glu191B-Met311A-His204B). The groups with Gln422B and Glu473B are themselves only connected by weak links and hence can be considered independent. The network itself shows an intricate coupling of residues of the X-loop and the tetra-helix bundle, the latter formed by TM3 and TM4 of both chains at the central axis of the "bottom-closed" holo structure. The Glu residue in position 473 has been shown to be conserved in ABC exporters [9] and has been suggested to play a role in transmitting conformational changes between the NBDs and the TMDs [32,33]. In our correlation network, Glu473B occupies a central position with the neighborhood of Met311A, Ser310A, Asn494A, Asn495A, and Gln116A. The symmetric equivalent residue, Glu473A is also present in the network connected with Met311B, Ser310B, Asn494B, Asn495B, and Asn126B. There is, however, an apparent asymmetry of internal connectivity between the neighborhoods of Glu473A and Glu473B, which might be a result of the inherent asymmetry of the Sav1866 X-ray structure. A number of residues in an asymmetric conformation can be found in this X-ray structure along the central axis of the transporter, including Asn102, Asn126, Gln200 and His204. The structural and dynamic asymmetry of the two chains could have a functional role as residues in this region are dynamically coupled to the X-loop of the NBDs.

The correlation network of the ATP/ADP system shows a simpler structure with weaker links and smaller groups indicating looser coupling between residues in general (Fig. 3B). Most importantly, the central role of Glu473B is diminished and taken by Gln422B. The cluster of Gln422A/B-Gln421A/B containing the ATP-sensing residues becomes coupled and linked to several residues of the coupling helices interacting with the NBD of chain B, in which ADP is bound. These correlations show an increased dynamic coupling of the NBDs with the coupling helices. The groups present in the ATP/ATP system are absent indicating the dynamic decoupling of the X-loops from the tetra-helix bundle. Such a decoupling can facilitate the disruption of the tetra-helix bundle, which has been shown to be an important step

in the transporter opening process in targeted MD simulations [15]. It is also notable that correlations with extracellular residues Met31A/B, Asn47B, His57B from TM1 and TM2 also vanish with nucleotide replacement.

Apart from the residues above, some others, such as Met311, Asn494, Asn495, Asn252 and Asp323, which have not been implicated before as crucial residues in the transport process, also seem to play important roles in the formation of dynamically correlated clusters. For instance, Met311 is strongly coupled to other residues in the ATP/ATP system and is located on TM6, which has been described as a main location for drug binding in multi-drug transporters [51–53].

These results show that a single nucleotide replacement in the NBD binding sites can cause a significant rearrangement in the correlated motions and dynamic coupling of the full transporter protein.

3.3. Increased flexibility in response to ATP hydrolysis

Conformational changes due to ATP hydrolysis have been extensively studied computationally in isolated NBD dimers [26,27,29–31], however, there has been only one study of hydrolysis related conformational changes in the whole transporter [54], where the post-hydrolysis state was modeled as both nucleotide binding sites containing ADP·Pi. As our correlation calculations show, even the hydrolysis of a single ATP molecule can alter the overall correlated motions in the whole transporter. Therefore, we studied the flexibility changes of the full transporter caused by the hydrolysis of a single nucleotide, modeled by our asymmetric ATP/ADP system.

The average root mean square fluctuation (RMSF) of each residue in the transporter was calculated separately for each trajectory. Similar to the method used in [55], we found it informative to calculate the average and the standard deviation of RMS fluctuation values for the different trajectories (Fig. 4). A large RMS value for a residue directly indicates increased flexibility. Moreover, a large variance of RMS values for different trajectories shows that multiple alternative conformational states with variable flexibility are available. Upon the modeled nucleotide hydrolysis, most regions in the transporter display flexibility characteristics similar to the ATP-bound state. The most significant change occurs in the helical subdomain of NBD in chain A, whose signature motif is in contact with ADP, In this chain, the outer three helices and the X-loop all gain flexibility. Other, more subtle effects of hydrolysis can be observed in the TMD of chain B, where transmembrane helices 3 through 6, and the flanked extracellular loop 3 all exhibit a larger variance of RMS values. Also, an increase in RMS variance is visible in TMH 1 and 2 of chain A. An increase in the variance of RMS values indicates that upon nucleotide hydrolysis, these regions can access states with increased flexibility. It should be noted that changes in flexibility in response to the replacement of a single nucleotide happen in an asymmetric fashion in the transporter.

3.4. A putative transition route from the holo to the apo conformation

Because of the lack of consensus on whether the dissociation of isolated NBD "dimers" happens in simulations with bound ATP or ADP, it is informative to view this scenario in a full length protein, Sav1866, in a lipid environment. In our simulations if ATP occupies both binding sites, no significant dissociation is observed. However, if the nucleotide is replaced by ADP in the binding site in chain B, both sites show more frequent deviations from the starting conformation (Fig. S2). This finding might indicate that nucleotide hydrolysis in the *cis* site also affects the *trans* site and causes loosened nucleotide binding. A similar observation, that the hydrolysis of ATP appears to be abrogated due to loosening of the interaction of the LSGGQ motif with the ATP, was found for the ATP/ADP bound MJ0796 system [26]. However, the maximum deviation of the two marker residues in our simulations is still only 4 Å, which does not indicate a well defined

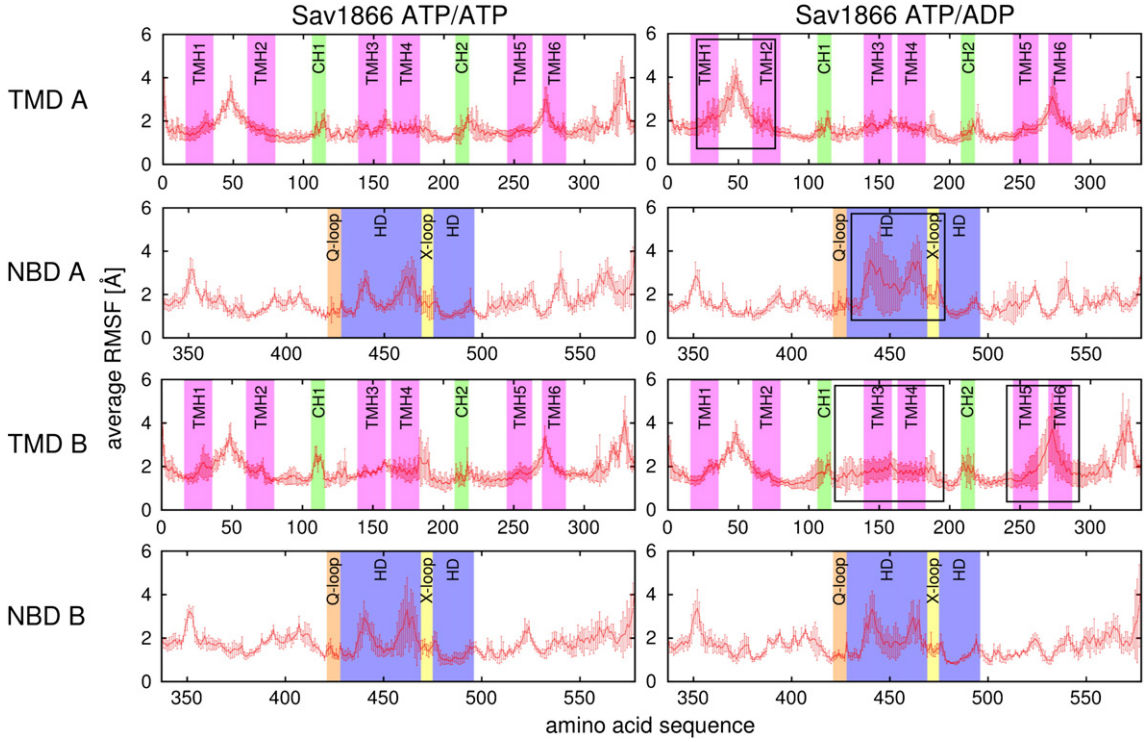

Fig. 4. Increased flexibility due to nucleotide replacement. The flexibility of the transporter is characterized by the RMS fluctuations for each amino acid around the average structure, calculated for all five trajectories. The error bars show the standard deviation of RMS values from different trajectories. The solid line represents the average RMS value. The replacement of a single nucleotide near the Walker A motif of NBD B, modeling ATP hydrolysis, causes a significant increase in flexibility in regions marked with boxes. Colors indicate important regions; yellow: X-loop, orange: Q-loop, blue: helical subdomain, green: coupling helices, magenta: transmembrane helices.

dissociation of the two domains. This could be attributed to the presence of the TMDs, which restrict the movement and dissociation of the NBDs.

Recently, a study by Becker et al. has shown that the transmembrane region can undergo spontaneous closure in the nucleotide-free state of the Sav1866 transporter [56]. Such a motion could be identified in one of our 100 ns ATP/ADP state trajectories, which could be a direct consequence of the increased flexibility of the transmembrane regions due to nucleotide replacement. To isolate and analyze the intrinsic collective motions in the transporter responsible for the transmembrane closure, we have analyzed the data from two trajectories of the ATP/ADP system, the one which exhibits closure, and the one which doesn't (simulations #2 and #1, respectively). Essential dynamics (ED) analysis of the atomic coordinates fitted on the common initial structure of the simulations was applied. This method is able to find low-frequency collective motions in a system, which have been shown to be functionally relevant [57–61]. In our case, the functionally relevant motion of transmembrane closure is already defined by trajectory #2, so the most relevant motions are expected to appear among the first few eigenmodes with the largest eigenvalues, corresponding to transmembrane closure. After essential dynamics analysis, the structures along both trajectories used in the analysis were projected along the first few eigenmodes (Fig. S3). The first eigenmode separates frames from the two trajectories well, which indicates that this motion is representative of the transmembrane closure transition. The separation between the trajectories diminishes with higher modes (Fig. S3). Based on this calculation, the first three eigenmodes (with the largest eigenvalues) were selected for further analysis. Our results indicate that the transmembrane closure on the extracellular side of the protein is coupled to a twisting sideways motion of the NBDs on the intracellular side (Fig. 5). The second and third largest amplitude modes also exhibit a sideways, although asymmetric motion of the NBDs in opposite directions (Fig. 5). Since these motions have been deduced from the analysis of the observed transmembrane closure, we believe that during the actual transport cycle, the dissociation of the NBDs initially involves a sliding and twisting motion of the domains relative to each other. Such a motion is not apparent from the comparison of the holo and "bottom-open" apo structures, and they could directly be able to switch the protein to the "bottom-closed" apo conformation (like the MsbA structure; PDB ID: 3B5X) without the large separation of the NBDs observed in the "bottom-open" X-ray structures.

3.5. The instability of the widely open apo conformation

One of our goals was to compare the dynamics of the holo and apo conformations of ABC transporters in molecular dynamics simulations. This attempt failed because the apo mouse MDR3 X-ray structure (PDB ID: 3G5U) exhibited instability in all our simulations. For a detailed analysis and characterization of the instability of the "bottom-open" conformation, we calculated the RMSD of the full length protein (Fig. 6A) and also for the TMDs and NBDs separately

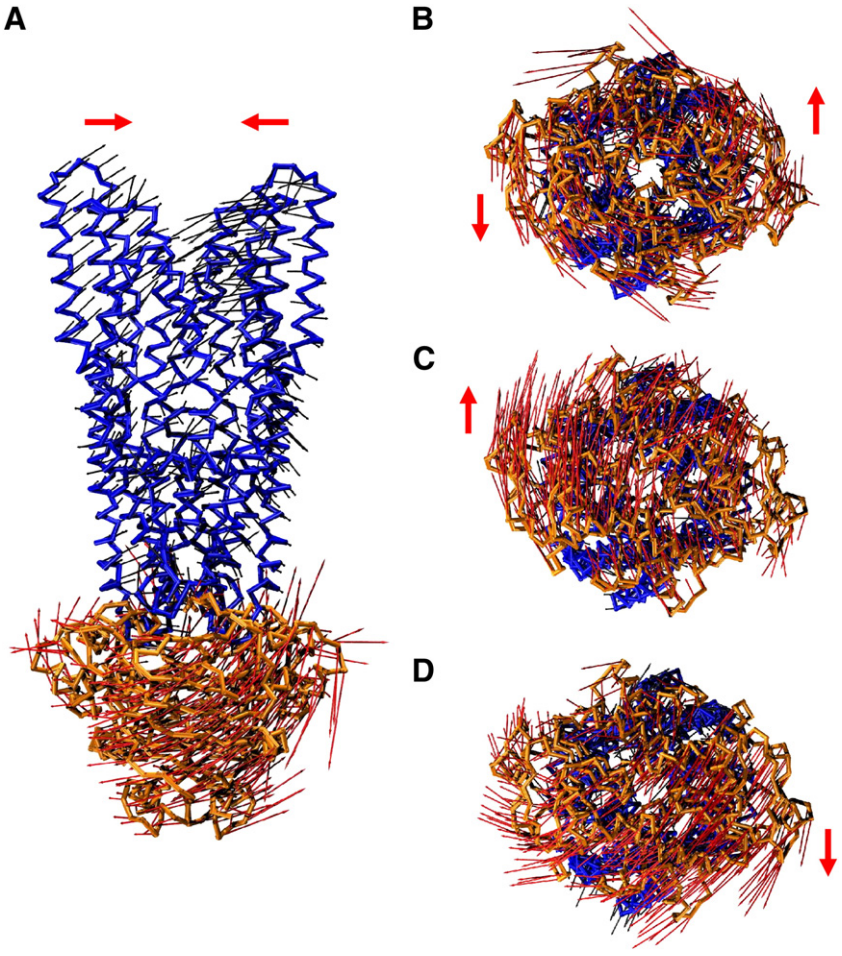

Fig. 5. Low-frequency essential dynamics (ED) modes define twisting motion of the NBDs coupled to the closure of the transmembrane helices. Essential dynamics analysis was used to separate the essential subspace of intrinsic motions where transmembrane closure can be observed. The first two panels show the atomic displacements along the first mode from (A) a side view of the transporter showing closure in the transmembrane region, and (B) a bottom view from the intracellular side showing a sliding and twisting motion of NBDs in opposite directions. The second (C) and third (D) modes also show rotational movements of the NBDs that could drive the system toward a conformation similar to that observed in the "bottom-closed" apo MsbA X-ray structure (PDB ID: 3B5X).

(Fig. 6B and C) over time with respect to the starting structure. A representative simulation with the double ATP bound Sav1866 was used as a reference for a stable "bottom-closed" holo conformation. The RMSD of the full length apo mMDR3 protein is much larger (~8–10 Å) than for a stable protein (Fig. 6A). The difference between RMSD values calculated separately for specific domains are smaller than for the full length protein. Fluctuations for the NBDs are between 3 and 4 Å compared to 2–2.5 Å for the Sav1866 ATP-bound system (Fig. 6B), and for the TMDs, ~6 Å compared to ~3 Å for the Sav1866 structure (Fig. 6C), respectively. The difference between RMSDs of the two structures is most pronounced in the TMDs. Analyzing the TMDs reveals that the most expressed instability of the "bottom-open" conformation is in the cytoplasmic, helical parts of the transmembrane domains (Fig. 6D). The increased flexibility of this region is the source of rigid-body movements of the NBDs and thus the cause of the highly increased RMSD of the full length protein. To characterize the increased flexibility and unwinding of the cytoplasmic parts of the TMDs, the helical content of the transmembrane domains was calculated from snapshots of the simulations. The average ratio of initially helical residues in the TMDs that remain dominantly helical during the simulations is only 75.61% as opposed to 90.04% for the Sav1866 simulations. This loss of secondary structure and the unwinding of cytoplasmic helices cause a detachment of the NBDs from the TMDs, indicating the instability of the interface and causing significant deformations in the structure. The same instability can be observed in all three simulations of the mouse MDR3 protein, and in simulations using various conditions (e.g. DPPC lipids; Fig. S4).

We find two plausible explanations for the instability of the "bottom-open" conformation. (1) The resolution of the X-ray structure is low, thus the orientation of side chains in the structure is not accurate. However, in this case, a general instability would be expected that is not localized to the intracellular loops. (2) The water accessibility of hydrophobic amino acids is increased in the "bottom-open" conformation. To test this hypothesis, we calculated the accessible surface area (ASA) of each residue in the intracellular loops of the mouse MDR3 protein using the CCP4 suite [48]. The accessible surface area (ASA) of non-polar and hydrophobic residues is listed in Table 2 for both the "bottom-closed" holo (homology model based on Sav1866) and "bottom-open" apo conformations. For simplicity, only residues exhibiting ASA at least twice as high in the "bottom-open" conformation as in the "bottom-closed" conformation (Table 2) and having an ASA of at least 20 $Å^2$ are considered. These residues were also plotted on the structures for visualization (Fig. S5). Most of these hydrophobic residues are located in the IL2 and in the corresponding coupling helix. For some amino acids, the difference of ASA in the two conformations is quite dramatic (increase of more than 10 times for Ala244, Leu254, Ala256, Phe789, etc.), while in other cases they are smaller but significant with relatively large absolute values (approx. 3–4 times larger ASA for Phe159, Leu283, and Phe900 with 124.1 $Å^2$, 105.3 $Å^2$, and 61.8 $Å^2$ in the "bottom-open" conformation, respectively). The ratio of the hydrophobic/hydrophilic accessible surface in the region of intracellular loops increased from 0.38 to 0.56 in the "bottom-open" conformation. Our calculation suggests that the source of the instability of the "bottom-open" conformation may indeed be the increased hydrophobic surface area.

4. Discussion

We performed MD simulations of ABC transporters embedded into a lipid bilayer to gather detailed information on the dynamic properties of various conformations along the catalytic cycle. First, we assessed if the ATP hydrolysis at one nucleotide binding site has an

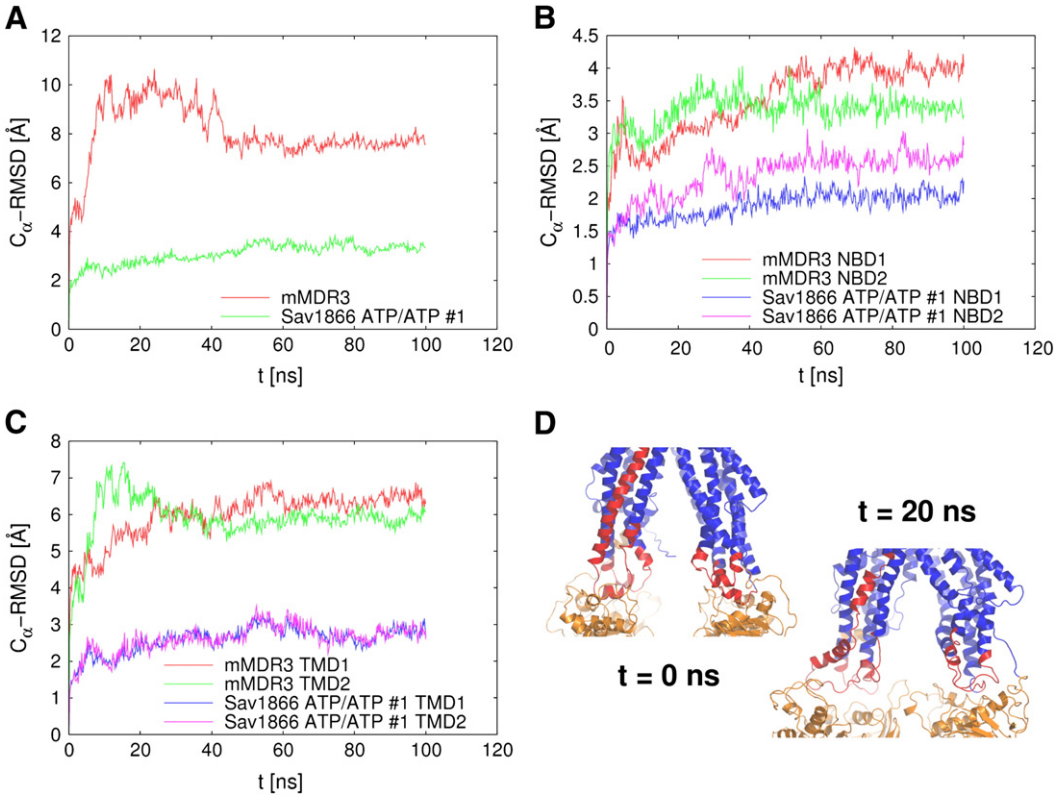

Fig. 6. Unstable segments in the "bottom-open" apo conformation. (A) The RMSD highly increased (8–10 Å) in the case of mouse MDR3, showing large deviations from the initial structure. As a stable system, values for a representative simulation with Sav1866 are also depicted. The increased RMSD of the apo MDR3 is caused by structural changes in the individual domains and rigid-body movements of the NBDs induced by the increased flexibility of the cytoplasmic parts of the TMDs. The NBDs (B) and the TMDs (C) also exhibit increased RMSD values. (D) The cytoplasmic parts of the TM helices in MDR3 are unwinding during the simulations indicating instability in these regions. Unstable regions are colored red.

Table 2
Differences in accessible surface area of selected residues from the "bottom-closed" holo and "bottom-open" apo conformations.

Region	Residue	ASA_{closed} [Å^2]	ASA_{open} [Å^2]
IL-1	PHE 159	28.7	124.1
IL-1	VAL 164	9.5	35.2
IL-1	GLY 165	6.8	35.2
IL-2	LEU 240	15.7	76.4
IL-2	ALA 242	3.9	27.3
IL-2	ALA 244	1.5	60.3
IL-2	ALA 248	6.7	58.6
IL-2	VAL 253	6.8	63.3
IL-2	LEU 254	5.0	51.1
IL-2	ALA 256	3.3	48.6
IL-2	VAL 260	5.6	21.0
IL-2	TYR 273	1.6	103.5
IL-2	LEU 277	6.8	44.9
IL-2	ALA 280	14.6	44.9
IL-2	LEU 283	34.0	105.3
IL-2	GLY 284	1.2	21.5
LINKER-1	ALA 352	6.5	49.8
LINKER-1	GLY 356	1.0	22.6
LINKER-1	ALA 357	2.5	26.7
LINKER-1	VAL 361	1.4	23.7
LINKER-1	ILE 364	9.1	91.3
LINKER-1	ILE 371	17	146.4
IL-3	PHE 789	2.5	24.1
IL-3	TRP 799	23.1	70.4
IL-3	GLY 808	0.7	32.7
IL-3	ALA 815	8.4	37.4
IL-4	ALA 879	10.5	38.1
IL-4	GLY 888	8.7	34.4
IL-4	PHE 900	15.8	61.8
IL-4	VAL 904	8.8	42.3
LINKER-2	VAL 999	3.0	90.2

The columns labeled ASA_{closed} and ASA_{open} display the accessible surface area (ASA) of residues from the "bottom-closed" holo and "bottom-open" apo conformations, respectively. IL is an abbreviation for intracellular loops, while LINKER denotes linker regions connecting the nucleotide binding and transmembrane domains. Only residues from the intracellular loops having an ASA twice as large in the "bottom-open" conformation than in the "bottom-closed" conformation and at least 20 Å^2 are shown.

overall effect on the dynamics of the whole ABC transporter. The gold standard "bottom-closed" holo conformation of Sav1866 was used to test the replacement of one of the ATP molecules with ADP. The analysis of mutual information of residues in both the ATP/ATP and ATP/ADP bound forms of the Sav1866 transporter showed that the simple replacement of ATP with ADP, when the energy of the γ-phosphate bond is not dissipated in the system, directly alters the network of dynamic interactions of residues. Residues in the Q-loops and X-loops which have been shown to have significant activity in signal transduction between NBDs and TMDs [32,33] appear as hubs in the dynamic correlation network of the ATP/ATP system (Fig. 3A). Interestingly, many of the correlations observed in the presence of two ATP molecules are absent in the ATP/ADP system (Fig. 3). This result suggests that ATP hydrolysis modifies the intrinsic dynamic pattern of the protein even without large structural changes. These alterations in dynamics then may lead to the subsequent destabilization of the NBD-NBD interface as well as several key NBD-TMD interactions, facilitating the transition of the transporter to the next step of the catalytic cycle.

We demonstrated that dynamic coupling exists between the TM3, TM6 helices and the nucleotide-bound NBDs. Based on these results, we suggest that key residues for function reside also in TM3. Interestingly, we note that extracellular residues that show dynamic coupling to the cytoplasmic regions are located between TM1 and TM2, in a longer extracellular loop, which is asymmetrically extended in human MDR1. This observation suggests a role for this loop in the asymmetric conformational changes during the catalytic cycle.

We also showed that the event of a single ATP hydrolysis modeled by ADP replacement alters the flexibility of certain parts of the transporter asymmetrically. In a very recent paper, Oliveira et al. have analyzed the effect of the replacement of both nucleotides with ADP·Pi, and were able to identify regions which change conformation due to nucleotide replacement [54]. Our results extend their work by showing that a single nucleotide replacement directly increases the flexibility of the helical subdomain and the X-loop in the *trans* NBD, as well as transmembrane helices 3 through 6 of the *cis* TMD in an asymmetric way. This suggest a possible pathway for the propagation of the hydrolysis signal from the nucleotide binding site via CH1 and the whole length of TMH 3, leading to the loosening of hairpin helices TMH 5–6 and TMH 1–2 from the *trans* chain. While a symmetric mechanism with double ATP hydrolysis might be a more natural model for a homodimeric transporter like Sav1866, such asymmetric effect of ATP hydrolysis could have great importance in eukaryotic transporters which have an asymmetric sequence, structure and variable length of extracellular loops.

A recent study of the ATP-bound and the nucleotide-free structures of the Sav1866 transporter by Becker et al. [56] reports that in the absence of nucleotides the transmembrane region of the structure undergoes closure on the extracellular side. Their analysis of the collective motions in the nucleotide-free structure revealed correlated motions between the cytosolic regions of TM3/TM4 and TM6. Interestingly, our ATP/ADP bound system showing the largest RMSD from the initial structure (system #2 on Fig. 2B) also exhibits closure on the extracellular side of the transmembrane regions (data not shown) as in the outward-facing, nucleotide-free system of Becker et al. [56]. This strikingly similar behavior of the ATP/ADP bound and the nucleotide-free states suggest that the hydrolysis of even a single ATP molecule could trigger closure of the transporter on the extracellular side and propagate the system towards the next step in the transport cycle. In spite of this, it should be noted that Stockner et al. [62] suggest that the conformation featuring TMD closure on the extracellular side could be accessible by thermal fluctuations. If occurring after ATP hydrolysis, this motion may contribute to the large basal ATPase activity of the transporter by facilitating the opening of the NBD interface. However, it is also possible that the extracellular closing motion due to thermal fluctuations imitates the effect of drug binding in the "bottom-closed" state and thus induces ATP hydrolysis.

Based on these results, we hypothesize that the "bottom-closed" ATP-bound form of the transporter is stabilized mainly by the tight coupling of the X-loop and the tetra-helix bundle. After the hydrolysis of a single ATP molecule, the coupling network of the X-loop, tetra-helix bundle, and the NBDs is mostly destroyed and replaced by the correlated motions of the coupling helices and the Q-loop. This change in the dynamics of the system is a key event, a signal from the NBDs back to the TMDs that, together with the closure of the extracellular gate, facilitate the opening on the cytoplasmic side. Unfortunately, because of the limited timescale of simulations with such a large system, the detailed mechanism and complete route of the conformational changes can not be followed, only residues possibly involved in these motions can be highlighted.

In several simulations with isolated NBD dimers [26–31], these domains have either opened or remained closed in the absence of ATP. Since our simulations with ATP/ADP bound Sav1866 did not show the dissociation of NBDs (Fig. S2), we predict a role for TMDs in constraining a relatively tight "dimer" configuration even in the absence of ATP. The tight coupling between NBDs and TMDs would favor the "bottom-closed" apo structure as a model for the apo state and thus might have implications for the extent of opening of the cytoplasmic side during the transport cycle. Substantial related experimental work on human MDR1 has been performed by Clarke et al. [25]. They have demonstrated that fixing the short distance between two helices corresponding to the "bottom-closed" conformation does not eliminate the ATPase activity of this protein. Their cross-linking experiments demonstrate that the existence of the "bottom-open" conformation may

not be obligatory for traversing the enzymatic transport cycle. Similar cross-linking experiments have been performed by van Veen et al. on the MsbA protein, capturing a difference in conformations in the presence and absence of ATP [63]. However, from their experiments it can not be concluded whether the NBDs move far apart. The absence of copper phenanthroline mediated cross-linking between cysteines inserted at position 208 in the two halves of cysteine-less MsbA may not necessarily originate from large conformational changes. In fact, in the "bottom-closed" MsbA structure, with NBDs close to each other, the two Glu208 are spatially separated by two helices. This conformation excludes the possibility of any type of cross-linking of these residues. Distance values from EPR experiments, lacking directional information, also can not answer the question whether the "bottom-closed" apo or the "bottom-open" apo structure is closer to the physiological conformation [10].

We analyzed the collective motions associated with spontaneous transmembrane closure in our asymmetric ATP/ADP system. In the first three modes with largest amplitude, we were able to observe a sideways displacement of the NBDs, happening in opposite directions, coupled to the closure of the transmembrane helices on the extracellular side. This coupling could imply that a sideways opening of the NBDs happens in tandem with the transition from the holo to the apo state of the transporter. We believe that after a hydrolysis event, this motion could drive the transporter directly towards a conformation resembling the "bottom-closed" apo structure observed in the case of the MsbA transporter (PDB ID: 3B5X). Based on these observations and the instability of the widely open apo structure, we believe that the "bottom-closed" apo conformation could be a physiologically more relevant model of the apo state than the widely open one.

The "bottom-open" mMDR3 structure was not stable in our simulations. Ivetac and Sansom have demonstrated [38] that molecular dynamics simulations can reveal incorrect packing in X-ray structures. An ABC transporter, the now revoked erroneous MsbA structure, was used as an example for exhibiting a significant structural instability on a short time scale. Although the "bottom-open" conformations in our simulations were not as unstable as the MsbA simulations, the apparent instability may indicate that the distance between the lower cytoplasmic parts of TMDs, thus also the distance between the NBDs, are not as large as in the X-ray structures. Our MD simulations also show that the large separation of the NBDs results in the detachment of the NBDs and the TMDs, which impairs the dynamic coupling of these domains, that is necessary for proper physiological function [33].

The instability may have different sources. First, because of the low resolution of the X-ray structure, the side-chain packing in mMDR3 may not be optimal, especially in the intracellular loops that show the highest level of instability. This also gives a warning that special attention is needed when relying on the orientation of side-chains, e.g. in interpreting drug-binding studies. Second, the water accessibility of non-polar and hydrophobic residues in the intracellular loops (Table 2), which are buried in the "bottom-closed" conformation, is increased. Such a conformation might be favored by the parameters of the crystallization environment (e.g. low temperature, absence of a lipid bilayer, etc.). This "bottom-open" conformation may also be stabilized in the crystal by the packing of the protein molecules. The widely open inward-facing conformation is observed in 3D crystals of MsbA (PDB ID: 3B5W) and mouse MDR3 (PDB ID: 3G5U), both of which contain more than one transporter per asymmetric unit cell. Although NBDs in one molecule are far from each other, these domains interact with the NBDs of neighboring molecules in the crystals (Fig. S6). These intermolecular NBD-NBD interactions present in all currently known widely open crystal structures do not happen at the canonical interaction ("dimerization") surface of these domains and seem to stabilize and constrain the widely open conformation. In contrast, the apo form of MRP1 in 2D crystals exhibits a slightly opened structure resembling the "bottom-closed" conformation [64]. Moreover, because of the high intracellular concentration of ATP (2–5 mM) compared to the K_M value of ATP (200–500 μM) we find it also possible that the widely open apo conformation is a short-living transient configuration captured under the crystallization conditions.

5. Conclusions

In summary, our results suggest that the hydrolysis of one ATP to ADP can lead to conformational changes which are part of the transport process (such as the closure of the extracellular parts of TMDs), thus supporting the alternating sites model of transport. Moreover, the instability of the "bottom-open" conformation does not simply emphasize the careful interpretation and application of 3D models, but also alludes to constantly interacting NBDs and strengthens the importance of the "bottom-closed" apo conformation. This apo conformation, as observed in MsbA X-ray structures, may serve as a better model for the post-hydrolytic state of exporter type ABC transporters, and could help in interpreting both experimental and computational results (such as mapping drug-binding sites and docking small molecules).

Acknowledgements

The authors wish to thank the Research Computing Facility of UNC at Chapel Hill for providing access to high performance computing resources.

Appendix A. Supplementary data

Supplementary data to this article can be found online at doi:10.1016/j.bbamem.2011.07.038.

References

[1] I.B. Holland, S.P.C. Cole, K. Kuchler, C.F. Higgins, ABC Proteins: From Bacteria to Man, Academic Press, NY, 2003.
[2] M.M. Gottesman, V. Ling, FEBS Lett. 580 (2006) 998–1009.
[3] G. Szakacs, A. Varadi, C. Ozvegy-Laczka, B. Sarkadi, Drug Discov. Today 13 (2008) 379–393.
[4] P.D. Eckford, F.J. Sharom, Chem. Rev. 109 (2009) 2989–3011.
[5] J.E. Walker, M. Saraste, M.J. Runswick, N.J. Gay, EMBO J. 1 (1982) 945–951.
[6] S. Wilken, G. Schmees, E. Schneider, Mol. Microbiol. 22 (1996) 655–666.
[7] P.C. Smith, N. Karpowich, L. Millen, J.E. Moody, J. Rosen, P.J. Thomas, J.F. Hunt, Mol. Cell 10 (2002) 139–149.
[8] J. Chen, G. Lu, J. Lin, A.L. Davidson, F.A. Quiocho, Mol. Cell 12 (2003) 651–661.
[9] R.J. Dawson, K.P. Locher, Nature 443 (2006) 180–185.
[10] I.D. Kerr, P.M. Jones, A.M. George, FEBS J. 277 (2010) 550–563.
[11] A. Ward, C.L. Reyes, J. Yu, C.B. Roth, G. Chang, Proc. Natl. Acad. Sci. U. S. A. 104 (48) (2007) 19005–19010.
[12] S.G. Aller, J. Yu, A. Ward, Y. Weng, S. Chittaboina, R. Zhuo, P.M. Harrell, Y.T. Trinh, Q. Zhang, I.L. Urbatsch, G. Chang, Science 323 (2009) 1718–1722.
[13] L.W. Hung, I.X. Wang, K. Nikaido, P.Q. Liu, G.F. Ames, S.H. Kim, Nature 396 (1998) 703–707.
[14] J. Aittoniemi, H. de Wet, F.M. Ashcroft, M.S. Sansom, PLoS Comput. Biol. 6 (2010) e1000762.
[15] J.W. Weng, K.N. Fan, W.N. Wang, J. Biol. Chem. 285 (2010) 3053–3063.
[16] T.W. Loo, D.M. Clarke, Arch. Biochem. Biophys. 476 (2008) 51–64.
[17] P. Zou, M. Bortolus, H.S. McHaourab, J. Mol. Biol. 393 (2009) 586–597.
[18] M. Grote, Y. Polyhach, G. Jeschke, H.J. Steinhoff, E. Schneider, E. Bordignon, J. Biol. Chem. 284 (2009) 17521–17526.
[19] B.A. Goetz, E. Perozo, K.P. Locher, FEBS Lett. 583 (2009) 266–270.
[20] M.A. Do Cao, S. Crouzy, M. Kim, M. Becchi, D.S. Cafiso, A. Di Pietro, J.M. Jault, Protein Sci. 18 (2009) 1507–1520.
[21] K.M. Westfahl, J.A. Merten, A.H. Buchaklian, C.S. Klug, Biochemistry 47 (2008) 13878–13886.
[22] A. Gustot, Smriti, J.M. Ruysschaert, H. McHaourab, C. Govaerts, J. Biol. Chem. 285 (19) (2010) 14144–14151.
[23] T.W. Loo, M.C. Bartlett, D.M. Clarke, J. Biol. Chem. 283 (2008) 28190–28197.
[24] T.W. Loo, M.C. Bartlett, D.M. Clarke, Biochemistry 46 (2007) 9328–9336.
[25] T.W. Loo, M.C. Bartlett, D.M. Clarke, Biochem. Biophys. Res. Commun. 395 (3) (2010) 436–440.
[26] P.M. Jones, A.M. George, Proteins 75 (2009) 387–396.
[27] P.M. Jones, A.M. George, J. Biol. Chem. 282 (2007) 22793–22803.
[28] P.M. Jones, A.M. George, Proc. Natl. Acad. Sci. U. S. A. 99 (2002) 12639–12644.
[29] S. Newstead, P.W. Fowler, P. Bilton, E.P. Carpenter, P.J. Sadler, D.J. Campopiano, M. S. Sansom, S. Iwata, Structure 17 (2009) 1213–1222.

[30] P.C. Wen, E. Tajkhorshid, Biophys. J. 95 (2008) 5100–5110.
[31] J.D. Campbell, M.S. Sansom, FEBS Lett. 579 (2005) 4193–4199.
[32] L. He, A.A. Aleksandrov, A.W. Serohijos, T. Hegedus, L.A. Aleksandrov, L. Cui, N.V. Dokholyan, J.R. Riordan, J. Biol. Chem. 283 (39) (2008) 26383–26390.
[33] G. Oancea, M.L. O'Mara, W.F. Bennett, D.P. Tieleman, R. Abele, R. Tampe, Proc. Natl. Acad. Sci. U. S. A. 106 (2009) 5551–5556.
[34] E.O. Oloo, D.P. Tieleman, J. Biol. Chem. 279 (2004) 45013–45019.
[35] J. Sonne, C. Kandt, G.H. Peters, F.Y. Hansen, M.Ø. Jensen, D.P. Tieleman, Biophys. J. 92 (2007) 2727–2734.
[36] A. Ivetac, J.D. Campbell, M.S. Sansom, Biochemistry 46 (2007) 2767–2778.
[37] A.E. Senior, M.K. al-Shawi, I.L. Urbatsch, FEBS Lett. 377 (1995) 285–289.
[38] A. Ivetac, M.S. Sansom, Eur. Biophys. J. 37 (2008) 403–409.
[39] D. Van Der Spoel, E. Lindahl, B. Hess, G. Groenhof, A.E. Mark, H.J. Berendsen, J. Comput. Chem. 26 (2005) 1701–1718.
[40] M.A. Marti-Renom, A.C. Stuart, A. Fiser, R. Sanchez, F. Melo, A. Sali, Annu. Rev. Biophys. Biomol. Struct. 29 (2000) 291–325.
[41] M.A. Larkin, G. Blackshields, N.P. Brown, R. Chenna, P.A. McGettigan, H. McWilliam, F. Valentin, I.M. Wallace, A. Wilm, R. Lopez, J.D. Thompson, T.J. Gibson, D.G. Higgins, Bioinformatics 23 (2007) 2947–2948.
[42] C. Globisch, I.K. Pajeva, M. Wiese, ChemMedChem 3 (2008) 280–295.
[43] G.E. Tusnady, I. Simon, Bioinformatics 17 (2001) 849–850.
[44] G.E. Tusnady, Z. Dosztanyi, I. Simon, Bioinformatics 21 (2005) 1276–1277.
[45] C.L. McClendon, G. Friedland, D.L. Mobley, H. Amirkhani, M.P. Jacobson, J. Chem. Theory Comput. 5 (2009) 2486–2502.
[46] W. Kabsch, C. Sander, Biopolymers 22 (1983) 2577–2637.
[47] B. Lee, F.M. Richards, J. Mol. Biol. 55 (1971) 379–400.
[48] N. Collaborative Computational Project, Acta Crystallogr. D. Biol. Crystallogr. 50 (1994) 760–763.
[49] C. Oostenbrink, A. Villa, A.E. Mark, W.F. van Gunsteren, J. Comput. Chem. 25 (2004) 1656–1676.
[50] A. Kukol, J. Chem. Theory Comput. 5 (2009) 615–626.
[51] T.W. Loo, D.M. Clarke, J. Biol. Chem. 271 (1996) 27482–27487.
[52] T.W. Loo, M.C. Bartlett, D.M. Clarke, J. Biol. Chem. 278 (2003) 13603–13606.
[53] J. Storm, M.L. O'Mara, E.H. Crowley, J. Peall, D.P. Tieleman, I.D. Kerr, R. Callaghan, Biochemistry 46 (2007) 9899–9910.
[54] A.S. Oliveira, A.M. Baptista, C.M. Soares, Proteins 79 (2011) 1977–1990.
[55] J.M. Damas, A.S. Oliveira, A.M. Baptista, C.M. Soares, Protein Sci. 20 (7) (2011) 1220–1230.
[56] J.P. Becker, F. Van Bambeke, P.M. Tulkens, M. Prevost, J. Phys. Chem. B. 114 (2010) 15948–15957.
[57] M. Kurylowicz, C.H. Yu, R. Pomes, Biophys. J. 98 (2010) 386–395.
[58] H.H. Loeffler, A. Kitao, Biophys. J. 97 (2009) 2541–2549.
[59] E.J. Beck, Y. Yang, S. Yaemsiri, V. Raghuram, J. Biol. Chem. 283 (2007) 4957–4966.
[60] O. Keskin, BMC Struct. Biol. 7 (2007) 31.
[61] L. Vaccaro, V. Koronakis, M.S. Sansom, Biophys. J. 91 (2006) 558–564.
[62] T. Stockner, S.J. de Vries, A.M. Bonvin, G.F. Ecker, P. Chiba, FEBS J. 276 (2009) 964–972.
[63] R. Doshi, B. Woebking, H.W. van Veen, Proteins 78 (14) (2010) 2867–2872.
[64] M.F. Rosenberg, C.J. Oleschuk, P. Wu, Q. Mao, R.G. Deeley, S.P. Cole, R.C. Ford, J. Struct. Biol. 170 (2010) 540–547.